Surface & Coatings Technology 329 (2017) 149–154

Contents lists available at ScienceDirect

Surface & Coatings Technology

journal homepage: www.elsevier.com/locate/surfcoat

Influence of reactive surface groups on the deposition of oxides thin film by atomic layer deposition

Riyanto Edy[a,b], Gaoshan Huang[b,*], Yuting Zhao[b], Ying Guo[c], Jing Zhang[c], Yongfeng Mei[b], Jianjun Shi[c,*]

[a] State Key Laboratory for Modification of Chemical Fibers and Polymer Materials, College of Materials Science and Engineering, Donghua University, Shanghai 201620, People's Republic of China
[b] Department of Materials Science, Fudan University, Shanghai 200433, People's Republic of China
[c] College of Science, Donghua University, Shanghai 201620, People's Republic of China

ARTICLE INFO

Keywords:
Atomic layer deposition
Reactive surface groups
Thin film

ABSTRACT

In this study, polyethylene terephthalate (PET) substrate was successfully coated Al_2O_3 and TiO_2 films by atomic layer deposition (ALD). The experiment results demonstrate that the Al_2O_3 can be deposited more efficiently than TiO_2 on PET substrates. Further characterization on the coated substrates reveals that the density of hydroxyl −OH groups play a significant role on the growth of the oxides ALD film. Chemical composition of the coated substrates is characterized by X-ray photoelectron spectroscopy, which shows that the C═O elements are replaced by the Al - related elements in the Al_2O_3 - coated PET and the Ti - related elements in the TiO_2 - coated PET. The results demonstrate that the C═O has a strongly contribution to facilitate the initial ALD growth of the oxides thin films.

1. Introduction

Atomic layer deposition (ALD) is an interesting technique for producing conformal inorganic thin films at relatively low temperatures [1,2]. Oxides thin films such as titanium oxide (TiO_2) attracts increasing interests due to its advantageous properties such as photocatalytic activity, photo-induced hydrophilicity, electron transport properties in solar cell applications, gas sensing, biocompatibility and optical properties [2–6]. ALD on polymers with lack of hydroxyl −OH groups is considered to be complicated in order to produce uniform layer and conformal film coverage without substantial subsurface growth [7,8]. For nucleation, the substrate must have reactive surface groups with which the precursor molecules can react to initiate ALD growth [9–11]. Hydroxyl groups on oxide surfaces are typical examples of such reactive groups [9,12,13]. In that case, the deposited thin film is chemically bonded to the substrate, and will therefore usually have a good adhesion [9]. In addition, the aluminum oxide (Al_2O_3) growth on the molecular porous polymeric substrates with lack of reactive groups was demonstrated to occur through the adsorption of the trimethylaluminum (TMA) precursor as initial nucleation period of 10–20 ALD cycles onto the surface or into the porous material leading to the formation of Al_2O_3 clusters [9,14,15]. In our previous study, it has shown that the deposited Al_2O_3 was amorphous with numerous reactive hydroxyl −OH groups [16]. The remarkable properties of Al_2O_3 that it was able to be deposited on a variety substrate at low temperature may have great potential applications [7,17,18]. In this study, it was shown that the reactive surface groups like hydroxyl −OH groups and −(C═O)−O− groups are necessary for ALD. Furthermore, it obviously indicates that Al_2O_3 ALD layer can be used as pre-treatment-like on polyethylene terephthalate (PET) surfaces to generate reactive surface hydroxyl −OH groups which can be used as the initial nucleation growth for the subsequent ALD.

2. Experimental details

In this study, polyethylene terephthalate (PET) and silicon were used as the substrates. The substrates were cleaned by an ultrasonic cleaner machine for 20 min with ultrasonic power and temperature of 80 W and 30 °C, respectively, which then were dried in the vacuum oven for 1 h at 50 °C. After that, Al_2O_3 and TiO_2 were deposited on the substrates by ALD with 100 cycles. For comparison, it was also prepared Al_2O_3/TiO_2 bilayer structure on the substrate with both materials of 100 ALD cycles. In ALD of TiO_2, Tetrakis (dimethylamido) titanium (TDMAT) and water vapor (H_2O) were sequentially exposed for 20 and 30 ms with purge times of 15 and 18 s, respectively. For ALD of Al_2O_3, TMA and H_2O were sequentially exposed with the same pulse and purge

* Corresponding authors.
E-mail addresses: gshuang@fudan.edu.cn (G. Huang), JShi@dhu.edu.cn (J. Shi).

http://dx.doi.org/10.1016/j.surfcoat.2017.09.047
Received 22 June 2017; Received in revised form 17 September 2017; Accepted 20 September 2017
Available online 21 September 2017

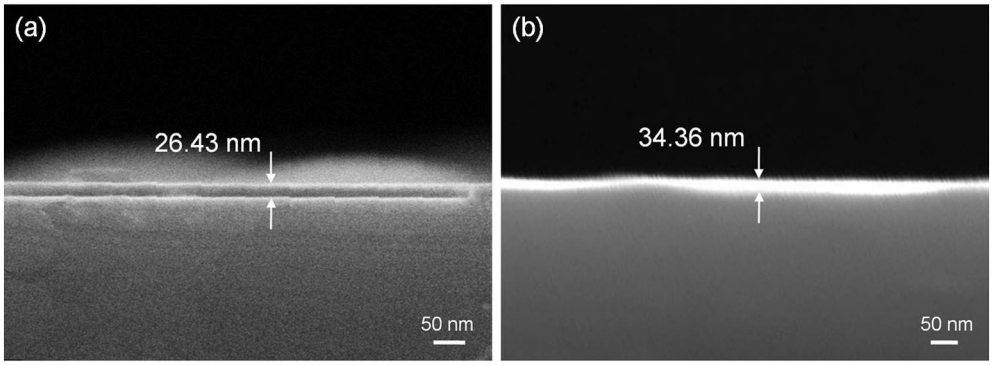

Fig. 1. Cross-sectional SEM images of silicon coated (a) Al_2O_3 and (b) TiO_2 films by ALD with 100 cycles.

times as used in the case of TiO_2. The deposition temperatures of Al_2O_3 and TiO_2 were 90 and 120 °C, respectively.

Cross section of the coated silicon and the surface view of the coated PET were imaged by a high resolution scanning electron microscopy (Magellan 400, FEI Company, USA). Atomic force microscopy (AFM; Nanoscope IV SPM, Model 920-006-101, Veeco Metrology, Santa Barbara, USA) was used to examine the surface morphology by using tapping mode. Wetting property of the surface was measured by a static contact angle analysis system (JC2000A, Powereach, Shanghai, China) and 0.4-μL droplet was used on each test. Chemical composition of the uncoated PET and the PET coated TiO_2 and Al_2O_3 films were evaluated by X-ray photoelectron spectroscopy (XPS).

3. Results & discussion

Fig. 1 show cross-sectional images of silicon substrates coated Al_2O_3 and TiO_2 films by ALD with 100 cycles (Fig. 1(a)–(b)). The SEM images demonstrate smooth surfaces with thicknesses of approximately 26.43 and 34.36 nm for Al_2O_3 and TiO_2, respectively. It implies that the parameters used in the ALD process are able to deposit the oxides thin films onto both silicon and PET, as the substrates are deposited in the same ALD reactor.

Fig. 2 show the SEM images of uncoated PET (Fig. 2(a)) and PET surface coated TiO_2, Al_2O_3, and Al_2O_3/TiO_2 bilayer films by ALD (Fig. 2(b)–(d)). The surface of PET without ALD film shows particle-like with wavy feature morphologies (Fig. 2(a)). The surface roughness reduces by presence the ALD film and it decreases significantly on the PET surface deposited by ALD with better film coverage (Fig. 2(c)–(d)). It was shown that PET surface coated Al_2O_3 film is smoother than that of TiO_2 film, which clearly indicates that the surface with Al_2O_3 has better film coverage than that of TiO_2 ALD. The smoothness of the PET surface can further increase by presence of Al_2O_3/TiO_2 bilayer film as shown in Fig. 2(d), which shows that the TiO_2 can be well grown onto the Al_2O_3 film acted as a buffer layer and the perfect coverage with regular ALD growth has been obtained as indicated by disappearing the wavy surface morphology.

Structurally, PET is a semi-crystalline polymer at room temperature which has functional groups of C═O as carbonyl site [16,19]. The presence of functional groups with Lewis base characteristics in polymer backbone makes the polymer reactive during exposure of precursor which is a strong Lewis acid [20,21]. Upon exposure of precursor, carbonyl site of the PET polymer coordinates with precursor (i.e. TMA, Lewis acid to form an aluminum-oxygen-alkyl unit) [21]. In Al_2O_3 ALD onto the PET substrate, a reaction forming a covalent aluminum-oxygen bond can proceed via methyl migration from TMA to the electrophilic carbon site of PET [19]. The possible reaction mechanism for TMA and H_2O reaction that the carbonyl stretch of C═O is eliminated by the TMA reaction with the carbonyl forming acetal group and a methyl transferred to the carbon of polymer backbone [19]. The subsequent water dose is likely to react with methyl in the acetal unit

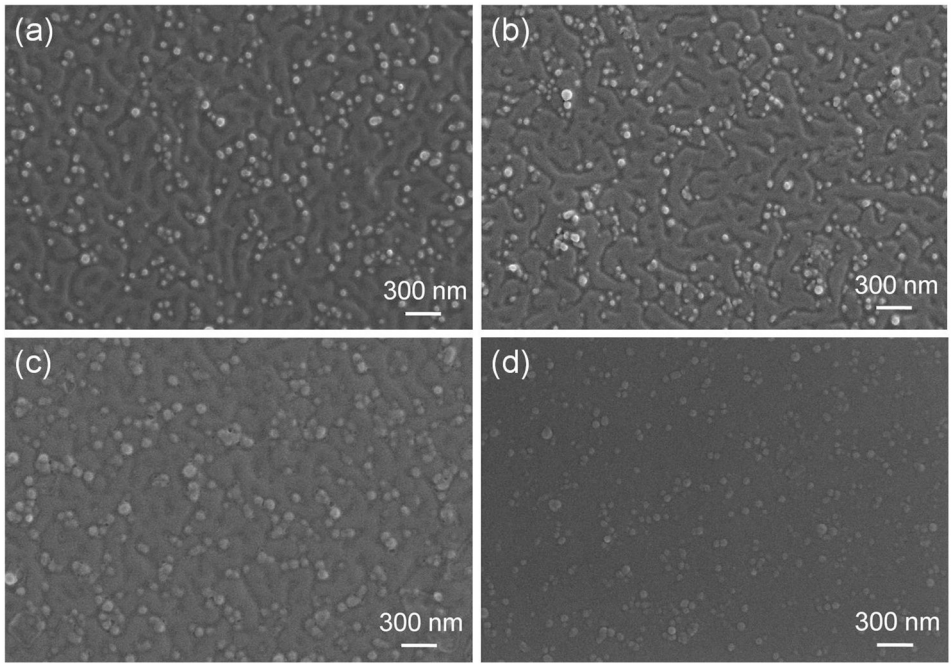

Fig. 2. SEM images of (a) uncoated PET and the PET surface coated (b) TiO_2, (c) Al_2O_3 by ALD with 100 cycles., (d) Al_2O_3/TiO_2 bilayer with both materials of 100 ALD cycles.

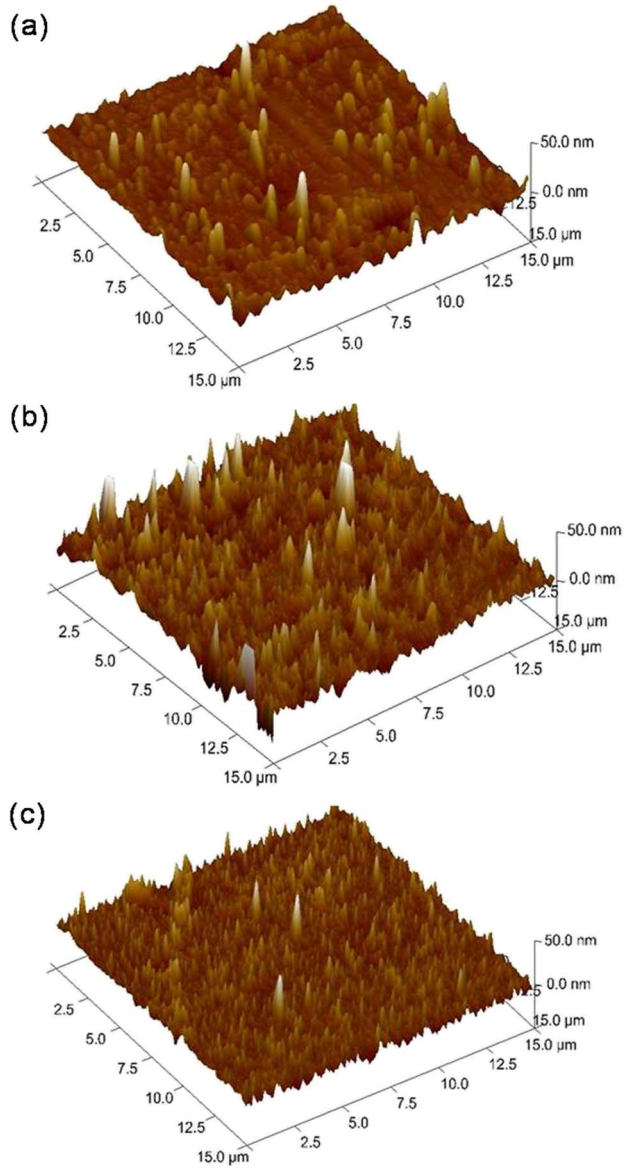

Fig. 3. Surface morphologies of (a) uncoated PET and the PET surface coated (b) TiO_2, and (c) Al_2O_3 films by ALD with 100 cycles.

forming −OH and releasing CH_4 as a product. The formed −OH groups can then be used to react with the subsequent precursor exposure. This growth mechanism lets the C═O to be replaced by the related elements of the ALD - grown oxide materials. The location of these carbonyl groups is expected mainly exist in the polymer subsurface. On the other hand, the coupling between precursor and carbonyl site can disrupt hydrogen bonding, resulting in the opening of the polymer chain framework, and this phenomenon able to further promotes the diffusion of precursor molecule into the subsurface region [21,22], which affects on the surface roughness. These typical ALD growth mechanisms can be indicated by surface morphologies evaluation before and after ALD coating.

Surface morphologies of the oxides deposited on PET were shown in Fig. 3. It reveals that the PET surfaces coated by ALD are smoother with more uniform morphologies than bald PET. The root mean square (RMS) surface roughness are evaluated to be 5.35 nm for bald PET surface which reduces to 5.05 and 3.75 nm for TiO_2 and Al_2O_3 films deposited on PET, respectively. It is an evidence suggesting normal growth of ALD has been achieved onto the surfaces of PET [16]. Since the ALD growth on polymers is strongly dependent on the nature of

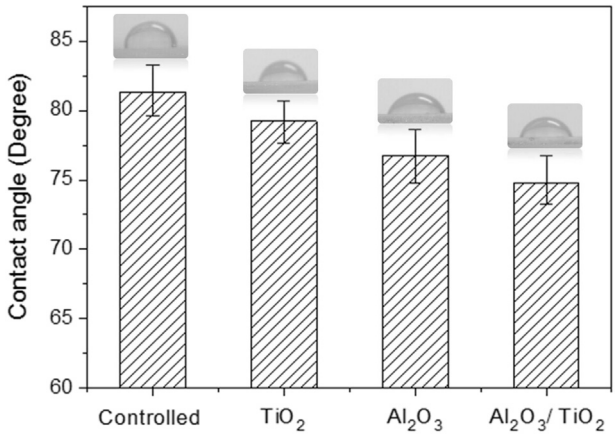

Fig. 4. Contact angles of uncoated PET and the oxides - coated PET.

polymer and on the ALD precursors [19,23], the current results indicate that the Al_2O_3 deposition used TMA precursor can be more efficient with better film coverage onto the PET surface. This phenomenon has an agreement to the SEM images evaluation which shows that the PET coated Al_2O_3 film by ALD is smoother than that of TiO_2 film as shown in Fig. 2(b) and (c).

Fig. 4 shows water contact angles of the uncoated and coated PET as a representation of surface wettability. The presence of hydrophilic oxygen-related functional groups, which act as primary to adsorp water molecules, increase wetting property of the surface and the water contact angle decreases correspondingly. The measurement demonstrates that the average water contact angle of the uncoated PET is 81.28° and reduces to 79.21, 76.78, and 74.79° for PET coated TiO_2, Al_2O_3, and Al_2O_3/TiO_2 bilayer films, respectively. It is worth noting that the water contact angle of PET coated Al_2O_3/TiO_2 bilayer film is lower than that of TiO_2 film. It indicates that the presence of reactive hydroxyl −OH groups with higher density on the Al_2O_3/TiO_2 bilayer surface can be the main reason for the hydrophilic improvement [24–26]. It can be explained that the initial functional hydroxyl −OH groups are provided on the surface for the next precursor exposure with the H_2O exposure on the Al_2O_3 surface [27,28]. The provided surface −OH groups on the Al_2O_3 layer can react with TDMAT molecules as initial growth and leading to the TiO_2 normal growth. The type of TiO_2 ALD growth onto Al_2O_3 is likely a substrate-inhibited ALD growth, the growth per cycle additionally goes through a maximum before settling to the constant value, which is caused by a lower number of reactive sites on the Al_2O_3 substrate than on the TiO_2 ALD-grown material [28–30]. These number are consistent with the fact that steric hindrance causes the amount of adsorbed ligands to be about constant and the required OH groups to release the ligands in the Al_2O_3 ALD reaction is lower than the TiO_2: three OH groups are needed to release the three methyl groups of one TMA molecule as CH_4, which attach one additional aluminum atom to the surface, and four OH groups are required to release the four $N(CH_3)_2$ groups of one TDMAT molecule as $NH(CH_3)_2$, which attach one titanium atom to the surface [28,29,31]. Those ligand exchange reactions are potentially able to gain the water compatible functional −OH groups with larger concentration on the Al_2O_3/TiO_2 bilayer surface. On the other hand, it is consistently shown that the water contact angle of sample coated with TiO_2 is higher than that with Al_2O_3, indicating that the TiO_2 is more difficult to be deposited than Al_2O_3. Furthermore, it implies that the Al_2O_3 film can be as buffer layer or pre-treatment-like by producing reactive hydroxyl −OH groups on surface to facilitate the subsequent ALD growth of materials which are challenging to be deposited.

Surface wettability is dependent on the chemical composition of the deposited oxides films, which is further probed by XPS spectra, and the results are shown in Fig. 5. Fig. 5(a) reveals the XPS spectra of C 1s of

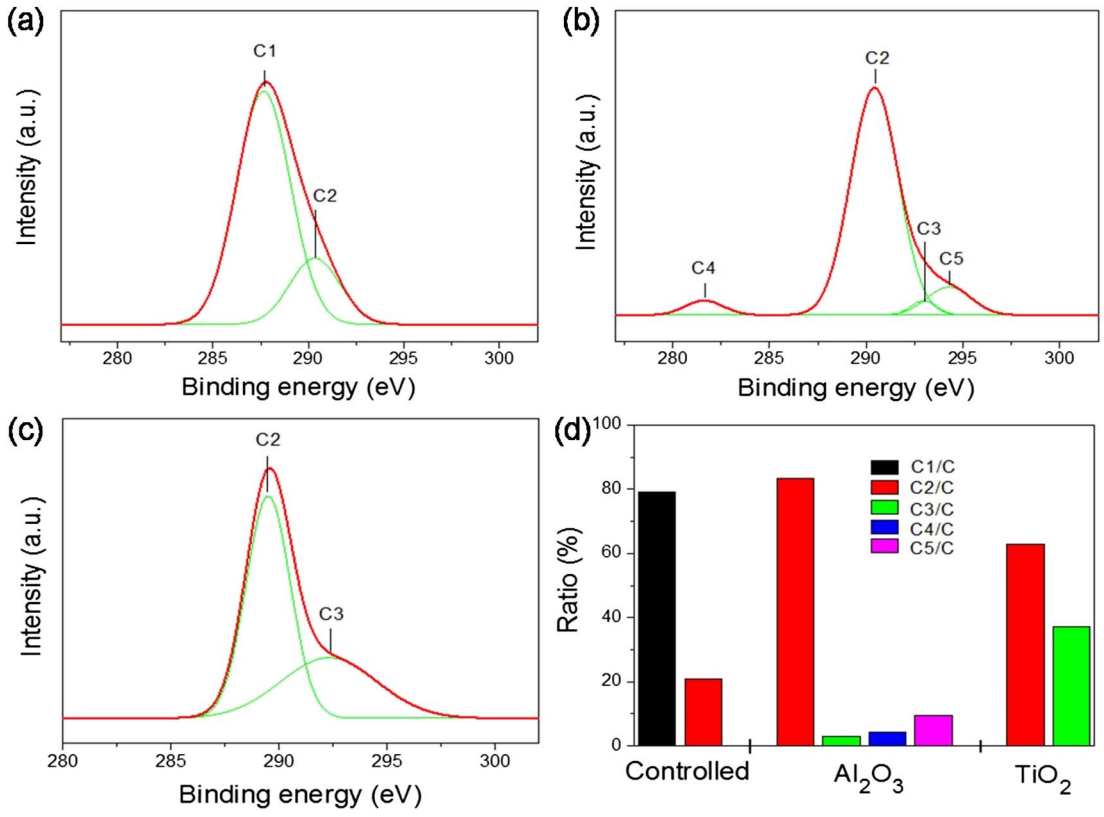

Fig. 5. XPS spectra of C 1s peaks of (a) uncoated PET, (b) the Al_2O_3-coated PET, and (c) the TiO_2-coated PET. (d) Relative elemental contents.

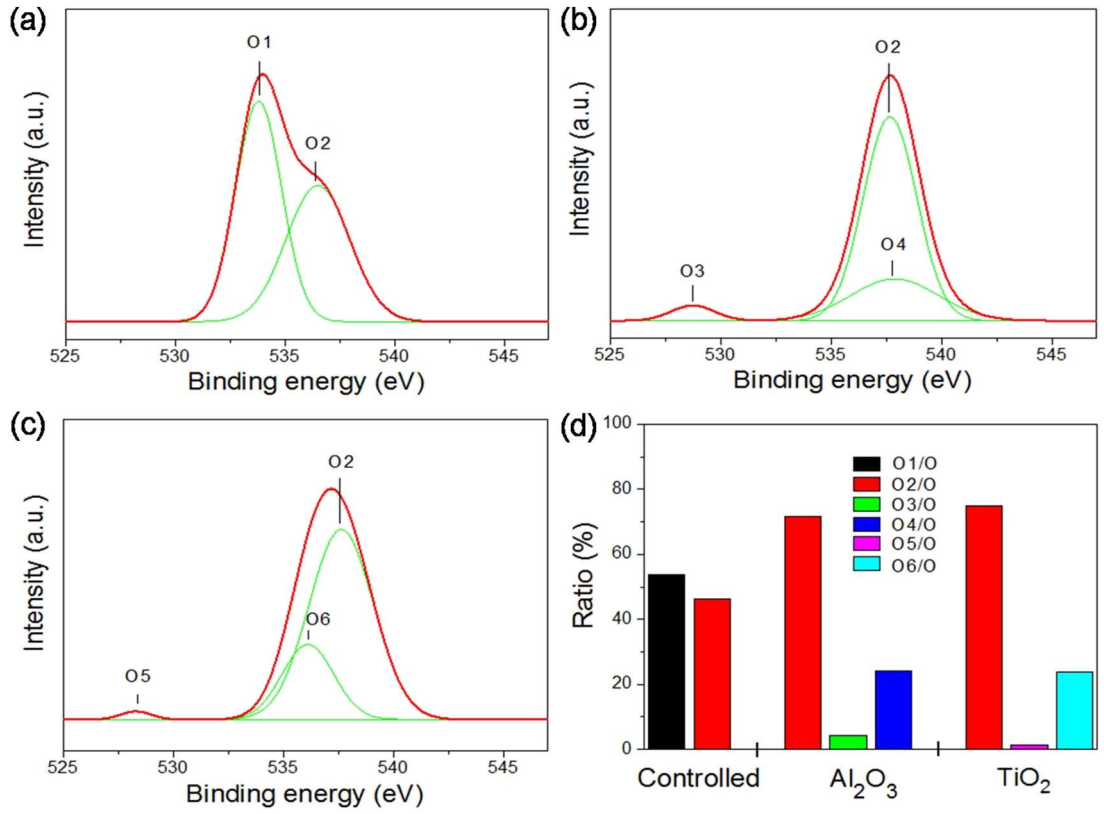

Fig. 6. XPS spectra of O 1s peaks of (a) uncoated PET, (b) the Al_2O_3-coated PET, and (c) the TiO_2-coated PET. (d) Relative elemental contents.

the uncoated PET. Two sub-peaks of C1 and C2 at 287.65 eV and ~289.96 eV, correspond to the −C−O, −C−C−, (and/or −C−R) and the −C═O, COOH, (and/or COOR), respectively [16,32]. In Fig. 5(b), the XPS spectra of Al_2O_3 - coated PET exhibits new peaks of C3, C4, and C5 at ~292.65 eV, 281.62 eV and 294.28 eV which correspond to the anhydride groups O═C−O−C═O, the C−O−Al, (and/or −H−C−Al) and the O═C−O, respectively [16,33,34]. The emergence of sub-peaks C3, C4, and C5 indicate new chemical states are formed in the Al_2O_3 - coated PET. On the other hand, a new sub-peak (C3) at 292.30 eV appears in the TiO_2 - coated PET, as shown in Fig. 5(c). Fig. 5(d) shows the elemental contents illustrated in Fig. 5(a)–(c). In addition, the concentration of the polar group in Al_2O_3-coated sample is even higher than that of the TiO_2-coated sample. The formation of polar groups including the hydroxyl groups in the oxides - coated PET is consistent with the wettability results shown in Fig. 4, in which the contact angles are reduced with oxide - coated PET.

Fig. 6(a)–(c) show the XPS spectra of O 1s peak of uncoated PET, Al_2O_3 - coated PET, and TiO_2 - coated PET samples, respectively. It shows that the spectrum of uncoated PET consists of O1 and O2 at the binding energies of 533.82 eV and ~537.10 eV, corresponding to C═O and C−O−, respectively [16,32,33]. In Fig. 6(b), the new peaks of O3 and O4 at 528.75 and 537.89 eV correspond to the Al_2O_3 (and O on AlO of AlOOH) and the Al_2O_3 (and Al−O−C), respectively [32,33]. While Fig. 6(c) shows the new peak of O5 and O6 at the binding energies of 528.31 eV and 536.13 eV, corresponding with the Ti−O bond (and/or −OH) in TiO_2 and the oxygen species of Ti−O−C, respectively [34,35]. The detailed relative O contents of the uncoated and the oxides - coated PET samples are shown in Fig. 6(d). It shows that the Al_2O_3 - coated PET sample consist of O2, O3, and O4, which suggests that the element of C═O is replaced by the Al - related elements like Al_2O_3, Al−O−C, and AlOOH. The TiO_2 - coated PET sample, on the other hand, consists of O2, O5, and O6, which suggests that the element of C═O is replaced by TiO_2, −OH in TiO_2, and the oxygen species of Ti−O−C. It obviously indicates that the polar groups of C═O can be contributed to facilitate the ALD initial growth of the oxides thin films to achieve a normal ALD growth, for both Al_2O_3 and TiO_2 deposition processes.

4. Conclusion

The successful deposition of Al_2O_3 and TiO_2 films onto the PET substrates were achieved by ALD which is demonstrated by alteration of the wettability property and chemical composition. Both the deposited Al_2O_3 and TiO_2 raise the wetting property of the surfaces. It was shown the feasibility of Al_2O_3 on the substrate lack of reactive hydroxyl −OH groups at low ALD temperature. It is also important to be noted that Al_2O_3 can be used as buffer layer for the deposition of TiO_2 film. This layer can act as a pre-treatment to obtain reactive −OH groups to facilitate the initial ALD growth for the subsequent material which is more difficult to be deposited. The characterization of chemical composition shows the formation of new elements of Al_2O_3, O in AlO of AlOOH, and Al−O−C in the Al_2O_3 - coated PET as well as the elements of the oxygen species of Ti−O−C, the Ti−O bond and −OH in TiO_2 in the TiO_2 - coated PET.

Acknowledgments

This work was funded by the Natural Science Foundation of China (Grant No. 11475043 and 11375042).

References

[1] M. Vähä-Nissi, M. Pitkänen, E. Salo, E. Kenttä, A. Tanskanen, T. Sajavaara, M. Putkonen, J. Sievänen, A. Sneck, M. Rättö, M. Karpinen, A. Harlin, Antibacterial and barrier properties of oriented poymer films with ZnO thin films applied with atomic layer deposition at low temperatures, Thin Solid Films 562 (2014) 331–337.
[2] T. Hirvikorpi, R. Laine, M. Vähä-Nissi, V. Kilpi, E. Salo, W.-M. Li, S. Linfors, J. Vartiainen, E. Kenttä, J. Nikkola, A. Harlin, J. Kostamo, Barrier properties of plastic films coated with an Al_2O_3 layer by roll-to-toll atomic layer deposition, Thin Solid Films 550 (2014) 164–169.
[3] R. Edy, Y.T. Zhao, G.S. Huang, J.J. Shi, J. Zhang, A.A. Solovev, Y.F. Mei, TiO_2 nanosheets synthesized by atomic layer deposition for photocatalysis, Prog. Nat. Sci.: Mater. Int. 26 (2016) 493–497.
[4] R. Edy, G.S. Huang, Y.T. Zhao, J. Zhang, Y.F. Mei, J.J. Shi, Atomic layer deposition of TiO_2-nanomembrane-based photocatalysts with enhanced performance, AIP Adv. 6 (2016) (115113(1–9)).
[5] S. Pan, Y.T. Zhao, G.S. Huang, J. Wang, S. Baunack, T. Gemming, M.L. Li, L.R. Zheng, O.G. Schmidt, Y.F. Mei, Highly photocatalytic TiO_2 interconnected porous powder fabricated by sponge-templated atomic layer deposition, Nanotechnology 26 (2015) (364001(6pp)).
[6] R. Edy, G.S. Huang, Y.T. Zhao, J. Zhang, J.J. Shi, Y.F. Mei, Aluminum-doped zinc oxide thin films synthesized by atomic layer deposition for photocatalysis, J. Mater. Sci. Eng. (2017) Article ID: 1673–2812. (0-0001-05, 2017 (Accepted)).
[7] J.D. Ferguson, A.W. Weimer, S.M. George, Atomic layer deposition of Al_2O_3 films on polyethylene particles, Chem. Mater. 16 (2004) 5602–5609.
[8] K. Lahtinen, T. Kääriäinen, P. Johansson, S. Kotkamo, P. Maydannik, T. Seppänen, J. Kuusipalo, D.C. Cameron, UV protective zinc oxide coating for biaxially oriented polypropylene packaging films by atomic layer deposition, Thin Solid Films 570 (2014) 33–37.
[9] M. Kemell, E. Färm, M. Ritala, M. Leskelä, Surface modification of thermoplastics by atomic layer deposition of Al_2O_3 and TiO_2 thin films, Eur. Polym. J. 44 (2008) 3564–3570.
[10] J.S. Jur, J.C. Spagnola, K. Lee, B. Gong, G.N. Parsons, Temperature-dependent subsurface growth during atomic layer deposition on polypropylene and cellulose fibers, Langmuir 26 (2010) 8239–8244.
[11] T.O. Kääriäinen, P. Maydannik, D.C. Cameron, K. Lahtinen, P. Johansson, J. Kuusipalo, Atomic layer deposition on polymer based flexible packaging materials: Growth characteristics and diffusion barrier properties, Thin Solid Films 509 (2011) 3146–3154.
[12] M. Vähä-Nissi, E. Kauppi, K. Sahagian, L.-S. Johanson, M.S. Peresin, J. Sievänen, A. Harlin, Growth of thin Al_2O_3 films on biaxially oriented polymer films by atomic layer deposition, Thin Solid Films 522 (2012) 50–57.
[13] Y. Xie, L. Ma, D. Pan, C. Yuan, Mechanistic modeling of atomic layer deposition of alumina process with detailed surface chemical kinetics, Chem. Eng. J. 259 (2015) 213–220.
[14] T. Hirvikorpi, M.V. Nissi, J. Nikkola, A. Harlin, M. Karppinen, Thin Al_2O_3 barrier coating onto temperature-sensitive packaging materials by atomic layer deposition, Surf. Coat. Technol. 205 (2011) 5088–5092.
[15] B. Gong, J.C. Spagnola, S.A. Arvidson, S.A. Khan, G.N. Parsons, Directed inorganic modification of bi-component polymer fibers by selective vapor reaction and atomic layer deposition, Polymer 53 (2012) 4631–4636.
[16] R. Edy, X.J. Huang, Y. Guo, J. Zhang, J.J. Shi, Influence of argon plasma on the deposition of Al_2O_3 film onto the PET surfaces by atomic layer deposition, Nanoscale Res. Lett. 8 (79) (2013) 1–9.
[17] M.D. Groner, F.H. Fabreguette, J.W. Elam, S.M. George, Low-temperature Al_2O_3 atomic layer deposition, Chem. Mater. 16 (2004) 639–645.
[18] C.D. McClure, C.J. Oldham, G.N. Parsons, Effect of Al_2O_3 ALD coating and vapor infusion on the bulk mechanical response of elastic and viscoelastic polymers, Surf. Coat. Technol. 261 (2015) 411–417.
[19] G.N. Parsons, S.E. Atanasov, E.C. Dandley, C.K. Devine, B. Gong, J.S. Jur, K. Lee, C.J. Oldham, Q. Peng, J.C. Spagnola, P.S. Williams, Mechanism and reactions during atomic layer deposition on polymers, Coord. Chem. Rev. 257 (2013) 3323–3331.
[20] Y. Xu, C.B. Musgrave, A DFT study of the Al_2O_3 atomic layer deposition on SAMs: effect of SAM termination, Chem. Mater. 16 (2004) 646–653.
[21] H.C. Guo, E. Ye, Z. Li, M.-Y. Han, X.J. Loh, Recent progress of atomic layer deposition on polymeric materials, Mater. Sci. Eng. C70 (2017) 1182–1191.
[22] J.C. Spagnola, B. Gong, S.A. Arvidson, S.A. Khan, G.N. Parsons, Surface and subsurface reactions during low temperature aluminum oxide atomic layer deposition on fiber-forming polymers, J. Mater. Chem. 20 (2010) 4213–4222.
[23] M. Napari, J. Malm, R. Lehto, J. Julin, K. Arstila, T. Sajavaara, M. Lahtinen, Nucleation and growth of ZnO on PMMA by low-temperature atomic layer deposition, J. Vac. Technol. A 33 (2015) (01A128-(1–7)).
[24] C. Huang, Y.-C. Chang, S.-Y. Wu, Contact angle analysis of low-temperature cyclonic atmospheric pressure plasma modified polyethylene terephthalate, Thin Solid Films 518 (2010) 3575–3580.
[25] C.X. Wang, M. Du, Y.P. Qiu, Influence of pore size on penetration of surface modification into woven fabric treated with atmospheric pressure plasma jet, Surf. Coat. Technol. 205 (2010) 909–914.
[26] R. Morent, N.D. Geyter, J. Verschuren, K.D. Clerck, P. Kiekens, C. Leys, Non-thermal plasma treatment of textiles, Surf. Coat. Technol. 202 (2008) 3427–3449.
[27] S.M. George, Atomic layer deposition: An overview, Chem. Rev. 110 (2010) 111–131.
[28] R.L. Puurunen, Surface chemistry of atomic layer deposition: a case study for the trimethylaluminum/water process, J. Appl. Phys. 97 (2005) (121301-121301-52).
[29] R.L. Puurunen, Analysis of hydroxyl group controlled atomic layer deposition of hafnium dioxide from hafnium tetrachloride and water, J. Appl. Phys. 95 (2004) 4777.
[30] R.L. Puurunen, A. Root, P. Sarv, M.M. Viitanen, H.H. Brongersma, M. Lindblad, A.O.I. Krause, Growth of aluminum nitride on porous alumina and silica through separate saturated gas-solid reactions of trimethylaluminum and ammonia, Chem. Mater. 14 (2002) 720–729.
[31] Q. Xie, Y.-L. Jiang, C. Detavernier, D. Deduytsche, R.L.V. Meirhaeghe, G.-P. Ru, B.-Z. Li, X.-P. Qu, Atomic layer deposition of TiO_2 from tetrakis-dimethyl-amido

titanium or Ti isopropoxide precursors and H_2O, J. Appl. Phys. 102 (2007) 083521.
[32] B.V. Christ, Handbook of Monochromatic XPS Spectra, XPS International, California, 2005.
[33] H. Ardelean, S. Petit, P. Laurens, P. Marcus, F. Arefi-Khonsari, Effects of different laser and plasma treatments on the interface and adherence between evapoated aluminium and polyethylene terephthalate films: X-ray photoemission, and adhesion studies, Appl. Surf. Sci. 243 (2005) 304–318.
[34] L. Zhi, Q. Xiangzhi, G. Xueping, Y. Cunzhong, F. Bin, Z. Weidong, Y. Xiangmin, Surface modification of the TiO_2 particles induced by γ irradiation, Nucl. Sci. Tech. 24 (2013) S010305.
[35] S.K. Sharma, X-Ray Spectroscopy, InTech, Croatia, 2012.